

# Earthquake scaling laws for creeping and non-creeping faults

Falk Amelung<sup>1</sup> and Geoffrey King<sup>2</sup>

Institut de Physique du Globe, Strasbourg, France

**Abstract.** The dependence of the summed moment release on the fault dimension differs between non-creeping faults and creeping faults or volcanic regions. This can be attributed to different earthquake scaling laws. The number  $N$  of events with fault length  $L$  scales for non-creeping faults as  $N(L) \sim L^{-2}$  and for creeping faults as  $N(L) \sim L^{-3}$ . This difference offers a means for mapping the distribution of creep in the seismogenic crust.

## Introduction

For many years the role of aseismic creep in the deformation of the seismogenic crust has been debated. Only in Central California has fault creep been unequivocally demonstrated to be important. Elsewhere creep has been inferred from an absence of large seismic events [e.g. *Jackson and McKenzie*, 1988], but limits of the historical earthquake records make such interpretations dubious. Using data from California we show that the scaling relations for small earthquakes in non-creeping and creeping regions are completely different and that small earthquakes can be used to detect creeping faults.

The size-frequency distribution of earthquakes is commonly described in terms of the  $b$ -value, the slope of the Gutenberg-Richter relation,  $\log N_c(M) = -bM + a$ , where  $M$  is the magnitude,  $N_c$  the cumulative number of earthquakes with magnitude  $>M$  and  $a$  a constant depending on the seismic activity [*Gutenberg and Richter*, 1954]. The  $b$ -value varies locally and regionally and can range between 0.5 and 1.5 [*Turcotte*, 1992; *Wiemer and Benoit*, 1996]. The most often observed  $b$ -value for crustal earthquakes is 1.0 [*Okal and Romanowicz*, 1994]. This paper describes a new approach to examining the size-frequency distribution of earthquakes. Instead of showing  $b$ -values, the summed moment release with respect to fault length (referred to as a moment-fault length distribution) is studied. To calculate this it is assumed that the earthquakes are self-similar with constant stress-drop. The analysis of moment-fault length distributions is under certain conditions mathematically identical to  $b$ -value analysis (see Appendix), but has the advantage of illuminating the geometric features of the earthquake process more clearly [*King*, 1983].

## Study area and data

In Central California (Fig. 1) most of the seismicity is related to right-lateral strike-slip faults. On some faults or fault segments the deformation is accommodated by brittle failure in large and destructive earthquakes, on other faults by aseismic creep or in a combination of both processes. The great 1906 San Francisco

earthquake ( $M7.7$ ) ruptured the 400 km long northern section of the San Andreas fault from Cap Mendocino (not shown in Fig. 1) to San Juan Bautista. The largest earthquakes since then were the 1983 Coalinga earthquake ( $M6.7$ ), the 1984 Morgan Hill earthquake ( $M6.3$ ) and the 1989 Loma Prieta earthquake ( $M7.0$ ) [*Ellsworth*, 1990]. In the south, the San Andreas fault creeps aseismically; the 150 km long fault segment between San Juan Bautista and Middle Mountain is widely referred to as the "creeping section" of the San Andreas fault. Other creeping faults are the southernmost segment of the Calaveras fault, the Hayward fault on its entire length but only at shallow depths and some portions of the Green Valley - Concord fault [*Galehouse*, 1992]. The creeping faults have continuous microearthquake activity.

The seismicity in Central California has been monitored since 1968 by the North California Seismic Network (NCSN). The earthquake catalogue is complete for events with magnitude  $M > 1.4$  [*Oppenheimer et al.*, 1990]. In order to study the distribution of moment release, the earthquake magnitude is converted to moment using the moment-magnitude relations  $\log M_0 = 1.5M - 1.5$  for events with  $M > 3.33$  and  $\log M_0 = 1.2M - 1.2$  for events with  $M \leq 3.33$  [modified from *Bakun*, 1984].  $M$  is the local or duration magnitude [*Eaton*, 1992], and  $M_0$  is the geometric moment, related to the seismic moment  $M_0$  by  $M_0 = \mu M_0$  [*King*, 1978; *Ben-Menahem and Singh*, 1981, p.179]. Here a

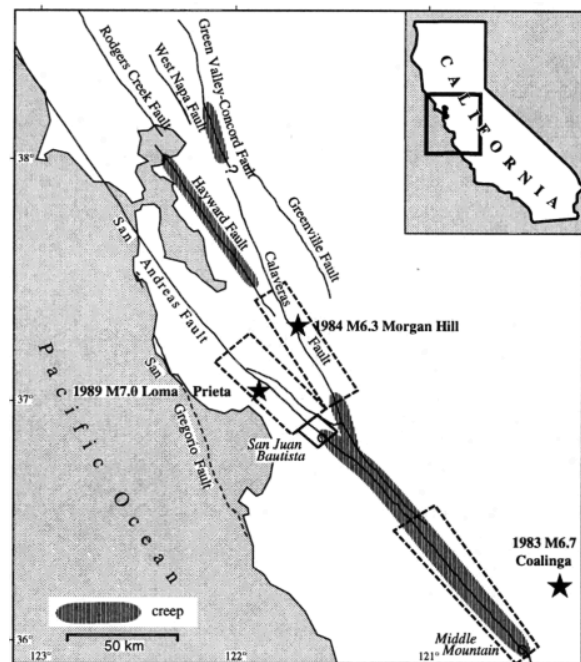


**Figure 1.** Location map showing the major faults, the creeping fault segments (shaded) and the epicenters of the major earthquakes (stars). The thick dashed and thick solid lines indicate regions that are discussed in Figs. 2 and 4, respectively.

<sup>1</sup>Now at GeoForschungsZentrum Potsdam, Germany

<sup>2</sup>Now at Institut de Physique du Globe de Paris, France

rigidity of  $\mu=30$  GPa is used. The relation for  $M > 3.33$  is equivalent to *Kanamori and Anderson's* [1975] relation between the seismic moment and the surface wave magnitude.

## Observations

In Fig. 2 the dependence of the summed moment release on the earthquake fault length is examined for two non-creeping faults; for the Calaveras fault that ruptured in the 1984 Morgan Hill earthquake and the fault that ruptured in the 1989 Loma Prieta earthquake, and for the southern part of the creeping section of the San Andreas fault. Each column represents the summed geometric moment of all earthquakes that occurred during a period of 28 years within a fault length interval indicated by the column width, equally spaced on a logarithmic axis [King *et al.*, 1994]. The fault length refers to the radius of a circular fault, related to the geometric moment by  $M_0 = 167 \Delta \epsilon L^3$  [Kanamori and Anderson, 1975]. The earthquake strain-drop  $\Delta \epsilon$  is the displacement to length ratio of an earthquake and related to the stress-drop by  $\Delta \sigma = \mu \Delta \epsilon$ . Throughout this study the strain-drop is assumed to be constant  $3 \cdot 10^{-4}$ , corresponding to a stress-drop of 10 MPa. The choice of logarithmic fault length intervals is useful because we expect power-law relations between the summed moment within a fault length interval,  $M_0^{\Sigma}(L)$ , and the fault length  $L$ .

On the Calaveras fault (Fig. 2A) and in the Loma Prieta area (Fig. 2B) the summed moment approximately doubles as the fault length doubles, i.e. the summed moment increases linearly with fault length. The relation  $M_0^{\Sigma}(L) \sim L$  is shown as a dotted line in figs. 2A and B. The major events of Morgan Hill and Loma Prieta do not fit this law, but this is to be expected because of their interaction with the free surface and the base of the seismogenic zone [e.g. *Pacheco et al.*, 1992]. In the creeping section of the San Andreas fault, however, a similar summed moment release is observed in all fault length intervals and the

moment-fault length distribution is approximated by  $M_0^{\Sigma}(L) = \text{const}$  (Fig. 2C). Note that the summed moment release of  $2.5 \cdot 10^6 \text{ m}^3$  in the southern creeping section of the San Andreas fault (80 km long) during a period of 28 years corresponds to a seismic slip rate of 0.1 mm/yr assuming a thickness of 12.5 km for the seismogenic upper crust. Hence, only 0.3% of the fault motion is seismic. On the non-creeping faults, on the other hand, the slip rate is dominated by earthquakes. The different moment-fault length distributions are also expressed as different  $b$ -values. For the Calaveras and Loma Prieta faults  $b$ -values of 0.9 and 0.8 are found, and 1.2 for the creeping section (Fig. 2). Theoretically, the moment-fault length distributions predict  $b$ -values (see Appendix) for non-creeping and for creeping faults of 1.0 and 1.5, respectively. The difference occurs because of the known difficulties in deriving  $b$ -values.

The above analysis is based on an empirical relation between  $M_0$  and  $M$ . Bakun's data, however, allow some variations of the parameters defining the moment-magnitude relations [Bakun, 1984, fig. 5]. The dashed horizontal bars in Fig. 2 are calculated using the relation for  $M < 3.33$  for all events regardless of their magnitude, and the solid horizontal bars are calculated changing from one relation to the other at magnitude  $M 2.5$ . The moment-fault length distributions are changed, but the basic difference between non-creeping (Figs. 2A and B) and creeping faults (Fig. 2C) remain unchanged. Our observations do not result from a fortuitous choice of the moment-magnitude relation.

In Fig. 3 the moment-fault length distributions all over Central California are analyzed. In some regions the distributions are similar to the Calaveras fault and to the Loma Prieta area, for example in the Livermore, Coalinga and San Francisco Peninsula regions and on the San Gregorio fault. The seismicity in the first three regions is related to faults that move in large earthquakes; to the Greenville fault that ruptured in the 1980  $M 6.0$  Livermore earthquake, to the Coalinga fault that ruptured in the 1983  $M 6.3$  Coalinga earthquake and to the San Andreas fault that ruptured in

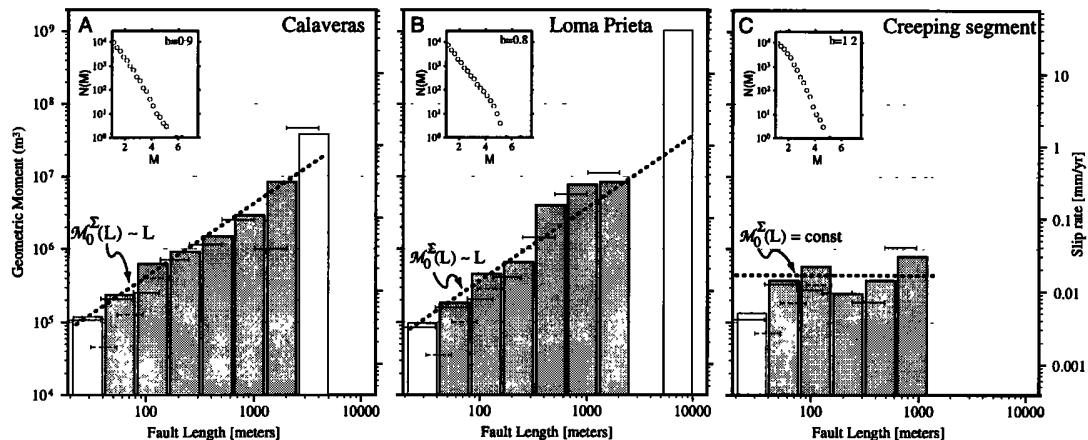


**Figure 2.** Summed geometric moment in different fault length intervals (A) on the Calaveras fault, (B) in the rupture area of the 1989 Loma Prieta earthquake and (C) on the southern creeping segment of the San Andreas fault. The regions are indicated in Fig. 1. The columns represent the total moment release within the magnitude intervals  $M 1.08-1.83$ ,  $M 1.83-2.58$ ,  $M 2.58-3.33$ ,  $M 3.33-3.94$ ,  $M 3.94-4.54$ ,  $M 4.54-5.14$ ,  $M 5.14-5.75$ ,  $M 5.75-6.34$  and  $M 6.34-7.0$ . The intervals are chosen such that the fault length varies from one magnitude interval to the next by a factor of 2. The fault length refers to a circular fault model assuming constant stress-drop. Since the moment-magnitude relation changes at magnitude 3.33 the abscissa is not linear in  $M$ . The major earthquakes and the magnitude intervals within which the earthquake catalogue is not complete are indicated by unshaded columns. The horizontal bars correspond to different moment-magnitude relations described in the text. The slip rate is for a seismogenic depth of 12.5 km and a 80 km long fault. The  $b$ -values are shown in the upperleft corners.

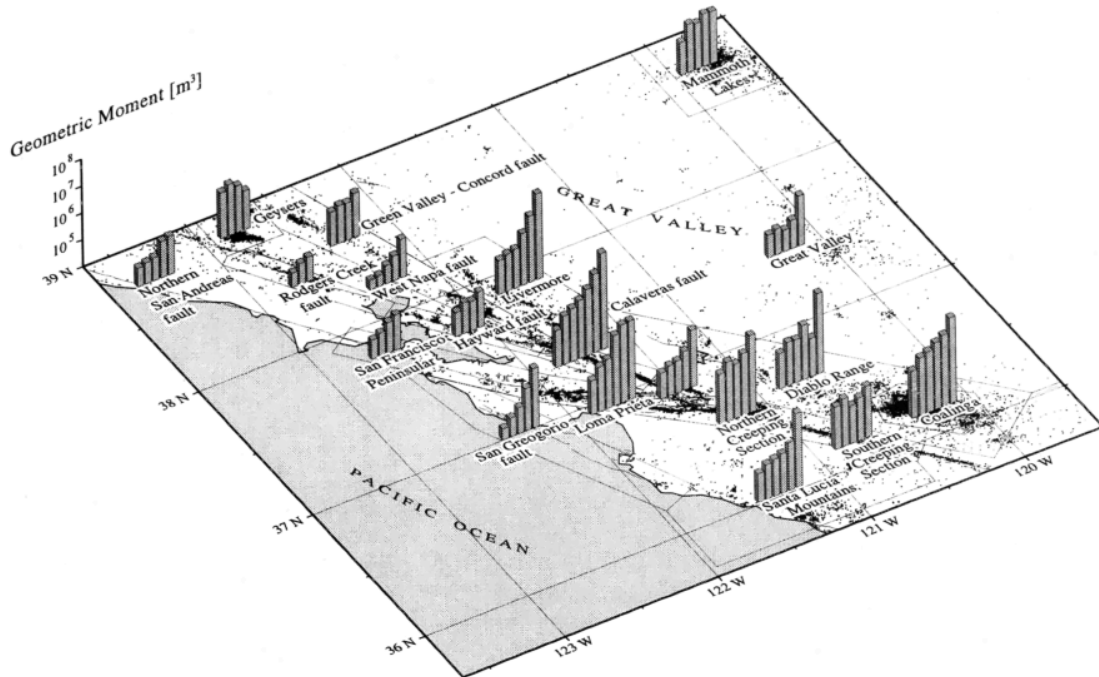


**Figure 3.** Moment-fault length distributions as in Fig. 2 but for different regions in Central California together with the seismicity ( $M > 1.5$ ) between 1969 and 1995. The first columns to the left represent the moment release in the  $M_{1.83-2.58}$  interval, the lowest magnitude interval in which the catalogue is complete.

the 1906 San Francisco earthquake. No historical earthquakes can be attributed to the San Gregorio fault [WGCEP, 1990], and this might be attributed to fault creep. The moment-fault length distribution, however indicates that this fault is non-creeping and therefore is potentially subject to future large earthquakes. Similar moment-fault length distributions are observed on the Rodgers Creek fault and in the region between the Rodgers Creek and the Green Valley faults that includes the West Napa fault. No creep has been detected on these faults [Galehouse, 1992] and the moment-fault length distributions indicate that they will be ruptured in large earthquakes.

The distributions on the Hayward and on the Green Valley-Concord faults are similar to those in the southern creeping section of the San Andreas fault. Both faults are creeping. In the

northern part of the creeping segment a slight increase of the total moment release with magnitude is observed. We note that this area contains the triple junction between the San Andreas and Calaveras faults and some non-creeping faults might exist at the junction. The distributions for the Geysers and Mammoth Lake regions are similar to that of the creeping section of the San Andreas fault. The seismicity in both areas is of volcanic or hydrothermal origin and the moment-fault length distributions should be different [King, 1983].

Up to now the moment release from a period of 28 years has been analyzed without distinguishing between background seismicity and aftershocks. Fig. 4 shows the summed moment release with respect to fault length in a sector of the San Andreas fault southeast of the rupture area of the 1989 Loma Prieta

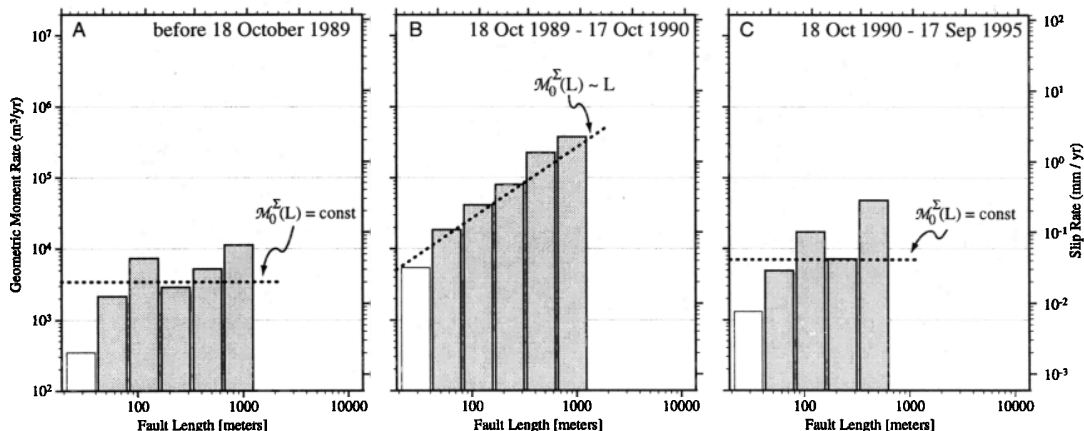


**Figure 4.** Moment-fault length distributions similar to Fig. 2 in a sector south of the rupture zone of the Loma Prieta earthquake. (A) Before the earthquake, (B) for one year of aftershocks and (C) for a subsequent 5-year period. The averaged rate of moment release per year is shown.

earthquake for three different time periods. For the period before the Loma Prieta earthquake the summed moment release is independent of fault length, indicating creep. For the 1-year period after the earthquake the summed moment release increases with fault length, indicating a non-creeping fault. During the subsequent 5 years, however, the summed moment release again is independent of fault length, indicating creep. These observations suggest that the distribution of the summed moment release with fault length of creeping faults depends on the loading rate. The earthquake slipped southeast of its epicenter primarily in strike direction and rapidly increased the shear stress and the slip rate on the creeping section of the San Andreas fault [Reasenber and Simpson, 1992]. The moment-fault length distributions became similar to a non-creeping fault until the stress increase was relaxed whereupon the typical moment-fault length distribution of a creeping fault was recovered.

## Conclusion

The dependence of the summed moment release on the fault length is systematically different between non-creeping and creeping faults. The total moment release increases on non-creeping faults linearly with the fault dimension,  $\mathcal{M}_0^{\Sigma} \sim L$ , and on creeping faults is independent of it,  $\mathcal{M}_0^{\Sigma} = \text{const}$ . This assumes that the earthquakes are self-similar and share the same stress drop. These observations can be restated as simple frequency-size scaling relations,  $N(L) \sim L^{-2}$  and  $N(L) \sim L^{-3}$ , respectively, since  $\mathcal{M}_0^{\Sigma}(L) = N(L) \mathcal{M}_0(L)$  and  $\mathcal{M}_0 \sim L^3$ , with  $N(L)$  the number of events (not the cumulative number) with fault length  $L$ . The frequency-size scaling for creeping faults changes to that of a non-creeping fault for increased loading rate.

It appears possible to use the moment-fault length distribution of microearthquakes to determine whether faults are creeping or non-creeping. An ability to distinguish between them using seismic information provides a potentially powerful tool for understanding the mechanics of the upper crust. This ability also has major implications for establishing seismic hazard. In Central California, for example, the moment-fault length distributions suggest that the San Gregorio fault is not creeping and that it can be the locus of a major earthquake.

## Appendix

The summed moment release,  $\mathcal{M}_0^{\Sigma}(L)$ , in a logarithmic fault length bin, given by

$$\mathcal{M}_0^{\Sigma}(L) = \int_{L/\sqrt{2}}^{L\sqrt{2}} \rho_L(L') \mathcal{M}_0(L') dL', \quad (1)$$

depends on  $\rho_L$ , the density distribution of the number of earthquakes with respect to  $L$ . The frequency of occurrence of earthquakes is commonly expressed in terms of the cumulative number of earthquakes  $N_c$  with magnitude  $\geq M$ ,  $N_c(M) = 10^{-bM+a}$ , where  $a$  and  $b$  are constants. The density distribution  $\rho_M$  of the number of earthquakes with respect to  $M$  defined by  $N_c(M) = \int_M^{\infty} \rho_M(M') dM'$ , is converted into  $\rho_L$  using  $\rho_L(L) = \rho_M(M)/(dL/dM)$ . Assuming that all the earthquakes share the same stress drop,  $\mathcal{M}_0 \sim L^3$ , and that  $\mathcal{M}_0$  relates to  $M$  by  $\log \mathcal{M}_0 = cM + \text{const}$ , the frequency of occurrence of earthquakes is given by  $\rho_L(L) = L^{-(\frac{3b}{c}+1)} \cdot \text{const}$ . Substituting into (1) gives the summed moment release in terms of the  $b$ -value,

$$\mathcal{M}_0^{\Sigma}(L) = L^{\frac{3-b}{c}} \cdot \text{const}. \quad (2)$$

The observations about the moment-fault length distributions,  $\mathcal{M}_0^{\Sigma}(L) = L \cdot \text{const}$  and  $\mathcal{M}_0^{\Sigma}(L) = \text{const}$  for non-creeping and creep-

ing faults, should be, in terms of the  $b$ -value for  $c=1.5$  [Kanamori and Anderson, 1975],  $b=1$  and  $b=1.5$ , respectively. If  $c$  is not the same for all magnitudes, as in the present study,  $\mathcal{M}_0^{\Sigma}(L)$  should vary with fault length, or the  $b$ -value should vary with magnitude. Thus, if the true scaling relations concern geometric or kinematic features of the earthquakes, then the  $b$ -value should be incorrect.

**Acknowledgments.** We are thankful to Dave Oppenheimer for helping us through the earthquake catalogue and to Chris Scholz for comments. F. A. was holding a doctorate grant from the European Union (EPOCH program). This research was supported by the CNRS.

## References

- Bakun, W. H., Seismic moments, local magnitudes, and coda-duration magnitudes for earthquakes in central California, *Bull. Seism. Soc. Am.*, 74, 439-458, 1984.
- Ben-Menahem, A. and J.J. Singh, *Seismic Waves and Sources*, 1108 pp., Springer-Verlag, New York, 1981.
- Eaton, J. P., Determination of amplitude and duration magnitudes and site residuals from short-period seismographs in northern California, *Bull. Seism. Soc. Am.*, 82, 533-579, 1992.
- Ellsworth, W. L., Earthquake history, 1769-1989, in *The San Andreas Fault System, California*, edited by R. E. Wallace, pp. 153-188, U.S. Geol. Surv. Prof. Pap., Washington, 1990.
- Galehouse, J. S., Creep rates and creep characteristics of eastern San Francisco Bay area faults, in *Second conference on earthquake hazards in the eastern San Francisco Bay area California*, edited by G. Borchardt, pp. 45-53, California Department of Conservation, 1992.
- Gutenberg B. and C. F. Richter, *Seismicity of the Earth and Associated Phenomena*, Princeton University Press, Princeton, 1954.
- Jackson, J. and D. McKenzie, The relationship between plate motions and seismic moment tensors, and the rates of active deformation in the Mediterranean and Middle East, *Geophys. J. Int.*, 93, 45-73, 1988.
- Kanamori, H. and D. L. Anderson, Theoretical basis of some empirical relations in seismology, *Bull. Seism. Soc. Am.*, 65, 1073-1095, 1975.
- King, G. C. P., Geological faults: fracture, creep and strain, *Phil. Trans. R. Soc. Lond.*, A. 288, 197-212, 1978.
- King, G. C. P., The accommodation of large strains in the upper lithosphere of the Earth and other solids by self-similar fault systems: the geometrical origin of the  $b$ -value, *Pageoph*, 121, 761-815, 1983.
- King G.C.P., D. Oppenheimer and F. Amelung, Block versus continuum deformation in the Western United States, *Earth Planet. Sci. Lett.*, 128, 55-64, 1994.
- Okal, E. A. and B. A. Romanowicz, On the variation of  $b$ -values with earthquake size, *Phys. of the Earth and Planet. Int.*, 87, 55-76, 1994.
- Oppenheimer, D. H., W. H. Bakun and A. G. Lindh, Slip partitioning of the Calaveras Fault, California, and prospects for future earthquakes, *J. Geophys. Res.*, 95, 8483-8498, 1990.
- Pacheco, J. F., C. H. Scholz, L. R. Sykes, Changes in frequency-size relationship from small to large earthquakes, *Nature*, 355, 71-73, 1992.
- Reasenber, P. A. and R. W. Simpson, Response of regional seismicity to the static stress change produced by the Loma Prieta earthquake, *Science*, 255, 1687-1690, 1992.
- Turcotte D. L., *Fractals and Chaos in Geology and Geophysics*, 221 pp., Cambridge University Press, Cambridge, 1992.
- Wiemer, S. and J.P. Benoit, Mapping the  $b$ -value anomaly at 100 km depth in the Alaska and New Zealand subduction zones, *Geophys. Res. Lett.*, 23, 1557-1560, 1996.
- Working Group on Californian Earthquake Probabilities (WGCEP), *Probabilities of large earthquakes in the San Francisco Bay region, California*, U.S. Geol., Surv. Circ. 1053, 1990.
- Falk Amelung, GeoForschungsZentrum, Telegrafenberg A31, D-14473 Potsdam, Germany. (e-mail: falk@gfz-potsdam.de)
- Geoffrey King, Institut de Physique du Globe, 4, Place Jussieu, 75252 Paris, Cedex 05, France. (e-mail: king@ipggp.jussieu.fr)

(Received September 3, 1996; revised November 28, 1996; accepted December 3, 1996.)